

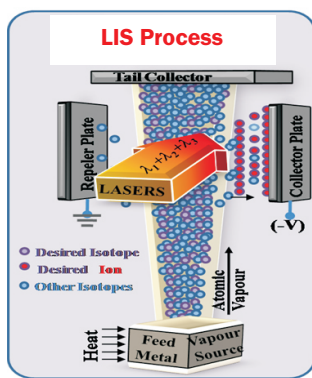
Isotope Separation

Analytical Approach to Understand Laser Isotope Separation Process of Yb-176 for Non Carrier Added (NCA) Radioisotope Lu-177

K. K. Mishra^{1*}, M. Mascarenhas¹ and Archana Sharma²

¹Laser and Plasma Technology Division, Beam Technology Development Group, Bhabha Atomic Research Centre, Mumbai-400085, INDIA

²Beam Technology Development Group, Bhabha Atomic Research Centre, Mumbai-400085, INDIA



LIS enrichment Process for Yb-176

ABSTRACT

Lutetium-177 (Lu-177) has emerged as a promising short range β -emitter for targeted radiotherapy. There are two ways to produce Lu-177. One is the Carrier Added (CA) method in which Lu-176 is used as a source material and second method is Non Carrier Added (NCA) wherein enriched Yb-176 is used as a source metal in nuclear reactor. Natural abundance of Yb-176 is only 13%, however the isotopic purity requirement of source material concentration is more than 95% of Yb-176. Laser Isotope Separation (LIS) method has been intensively used worldwide to produce high enriched Yb-176 (more than 95%) in weighable amount (10-20 mg/hr). At Bhabha Atomic Research Centre (BARC), multiple experiments for LIS of Yb-176 have been conducted in RIS facility of BTDG. Yb-176 enriched to 97.1% with Yb-174 1.09% has been obtained at mass production rate 5 to 10 mg/hr. In this paper a mathematical model of the LIS process applicable for high enrichment factor with mg quantity as required for medical isotopes is presented. Data generated from the model was compared with experimental results.

KEYWORDS: Lutetium-177, Carrier Added (CA) Method, Laser Isotope Separation (LIS), Non Carrier Added (NCA) Method, LIS Process, Yb-176, Enrichment of Yb-176.

Introduction

Lutetium-177 (Lu-177) has emerged as a promising short range β -emitter for targeted radiotherapy[1-2]. Demand of Lu-177 has increased many folds. Lu-177 is produced [3-5] in a nuclear reactor through irradiation of source material with neutrons. Currently, there are two ways to produce Lu-177. One is Carrier Added (CA) method in which Lu-176 used as a source material and second method is Non Carrier Added (NCA) where in enriched Yb-176 used as a source metal in nuclear reactor. Due to chemical difference between Lu-177 and Yb-176 carrier free Lu-177 is possible by separating Lu-177 from Yb-176 chemically. Natural abundance of Yb-176[6] is only 13%, however the isotopic purity requirement[7] of source material concentration is more than 95% of Yb-176 and less than 5% of Yb-174 (natural abundance 32%) to produce high activity Lu-177 in nuclear reactor.

Laser Isotope Separation (LIS) method[8-9] has been intensively used worldwide to produce high enriched Yb-176 (more than 95%) in weighable amount (10-20 mg/hr). At Bhabha Atomic Research Centre[10-11] extensive work has carried out for various isotopes. With this experience and utilization of RIS facility of Beam Technology Development Group in BARC multiple experiments for LIS of Yb-176 have been conducted. Enriched Yb-176 97.1% with Yb-174 1.09% has been obtained at mass production rate 5 to 10 mg/hr. In literatures various physical aspects of LIS process are already discussed.

*Author for Correspondence: K. K. Mishra
E-mail: kkmishra@barc.gov.in

The aim of this paper is to present a mathematical model of the LIS process applicable for high enrichment factor with mg quantity as required for medical isotopes. Model is based on isotropic mass balance and change of isotropic concentration of target isotope with controllable process parameters. The outcome of this calculation such as enrichment factor and mass of enriched Yb-176 is compared with the plant data obtained in RIS facility.

In LIS process, atoms of target isotope (Yb-176) in vapor stream get ionized after interaction with tuned laser beam. Ionized atoms are separated from the main vapor stream by electrostatic field. In the RIS facility a resistive heating system has been designed to evaporate Ytterbium by sublimation at temperature in the range of 780K to 820K to provide adequate Yb vapor atoms for laser interaction. The in house dye laser pumped by cover vapor laser (CVL) and Diode Pumped Solid State Laser (DPSSL) has been developed to selectively ionize Yb-176. Extraction mechanism of charged isotope Yb^+ -176 has been designed [12] in house.

Evaporation and Free Jet Expansion from a Rectangular Slit

During the process, the linear vapor jet coming out from a crucible at pressure (10–20 Pa) freely expands into vacuum chamber of pressure 10^{-3} Pa. As pressure ratio (source/background) is higher than critical ratio $[(\gamma+1)/2]^{1/(\gamma-1)} = 2.05$ (from gas dynamics), the vapor jet comes out from source reach to sonic speed at the exit plane, then it expand supersonically into vacuum. Properties of vapor at source as well as at a height are discussed below.

Vapor Pressure of Yb metal [13] is given by

$$\text{Log}_{10}P_0 = 14.117 - 8111/T_0 - 1.0849 \text{Log}_{10}T_0 \quad (1)$$

(Where P_0 in Pa)

Number density at source is calculated from ideal gas equation as

$$n_0 = \frac{P_0 A_v}{T_0 R_0} = \frac{P_0}{kT_0} \quad (2)$$

Average thermal velocity of atom from kinetic theory of gas is given by

$$V_{th} = (8RT_0/\pi)^{0.5} \quad (3)$$

Knudsen number[14-15] is the ratio of mean free path of atom to the dimension of source. It is an important parameter of the vapor source which governs flow dynamics of vapor jet issuing out from reservoir. The Knudsen number at source influences the atomic properties of vapor at atom-laser interaction zone. Mathematically it is given by Eqn. 4

$$kn_0 = \frac{\lambda}{w} = \frac{1}{1.414x\pi d^2 n_0 w} \quad (4)$$

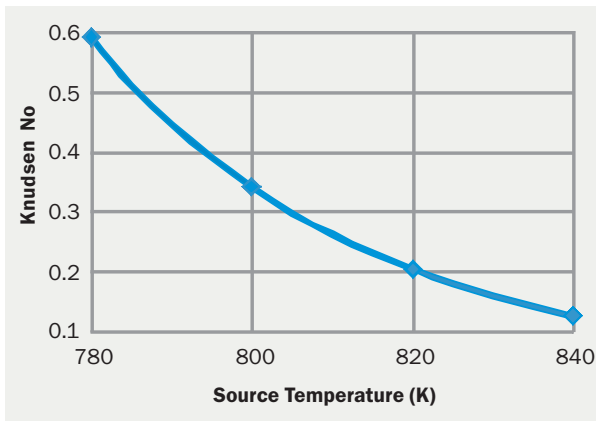


Fig.1: Variation of source Knudsen No with temperature.

It is seen from Fig.1 that Knudsen number remains in between 0.3-0.2 during evaporation of Yb in operating temperature range 800-820K. This is the transition regime of vapor flow where continuum gas flow equations[14] do not apply. Hence, continuum properties of free jet expansion is not discussed in this paper. In is model, vapor jet properties after expansion are calculated by using analytical equations derived by Monte Carlo particle test method for three dimensional non-collisional flow from a rectangular slit[16].

Number density[16] at height r from source plane

$$n_r = n^* \times (w/L) \times n_s \quad (5)$$

Where, n_s is number density at sonic plane of source[15] given by

$$n_s = (2/\gamma + 1)^{1/(\gamma-1)} n_0 = 0.65n_0 \quad (6)$$

and n^* is the geometric expansion factor[16] decides change in number density with height and is given by

$$n^* = \{[(1+(L/r)^2)^{0.5} - 1]/(2\pi)\} \quad (7)$$

Variation of number density during process at different location is shown in Fig.2. Number density at atom-laser interaction zone comes down by three orders from source.

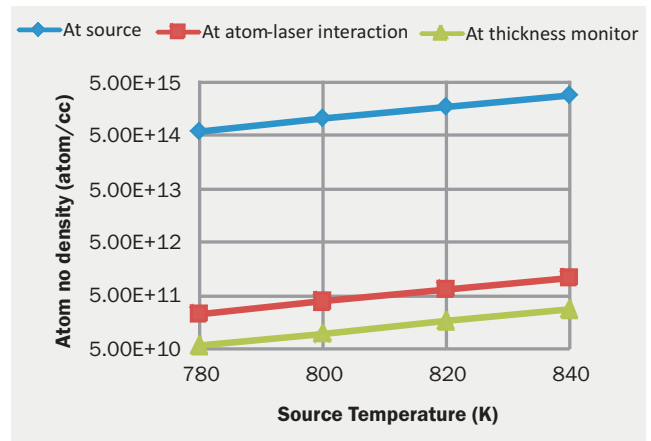


Fig.2: Variation of number density (Eqn.5) at various locations with source temperature.

Estimation of Thickness Monitor Data

Thickness monitor reading gives average arrival rate of atomic vapor in terms of thickness per unit time (A/sec). Product of mass density and thickness rate gives mass flux of metal vapor. Mass flux is also the product of number density of atom and its average velocity. Equating equation of mass flux

$$S_p = (M/A_v) n_r v_{th} \quad (8)$$

Where, n_r is number density of Yb atoms striking at the thickness monitor. Since, at a larger height velocity of atom reaches v_{th} , calculated at source temperature.

After substituting the values of constant and material properties thickness rate for Yb atoms comes to

$$S = 4.17 \times 10^{-11} n v_{th} \text{ A/sec} \quad (9)$$

Where, n from Eqn.5 in atom/cc and v_{th} from Eqn.3 in m/s.

Matching of experimental and theoretical data for thickness monitor provides an additional check to get the accurate number density of vapor atoms in atom-laser interaction zone.

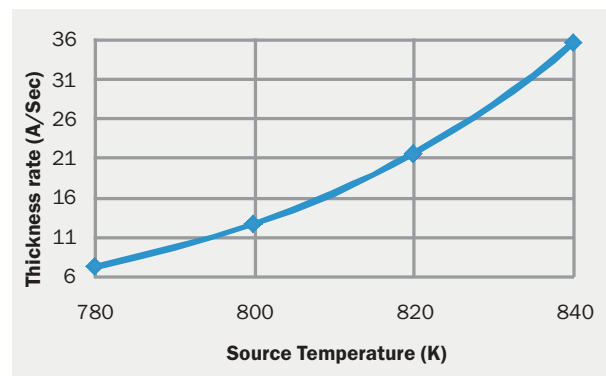


Fig.3: Variation of thickness monitor reading with source temperature.

Mass Balance and Enrichment Factor During LIS Process

Mass flow during LIS process is described in Fig.4

For total mass balance

$$F = P + W \quad (11)$$

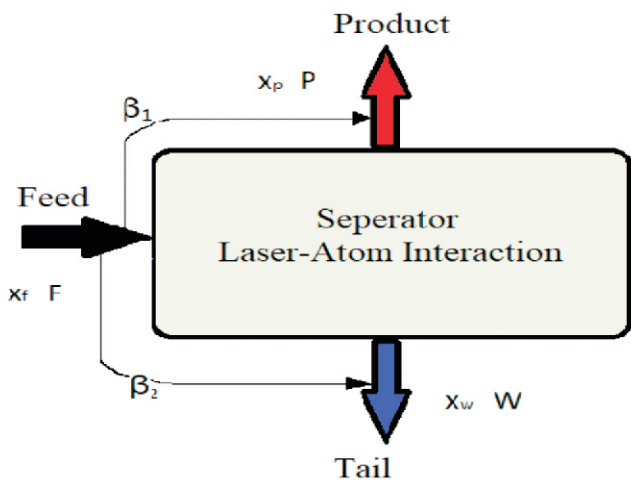


Fig.4: Mass flow during LIS process.

For Yb-176 mass balance

$$x_f F = x_p P + x_w W \quad (12)$$

Where, feed is given by Eqn.13 and its variation with source temperature is presented in Fig.5

$$F = (nV/t)(M/A_v) = 5.1727E-10 \text{ n mg/hr} \quad (13)$$

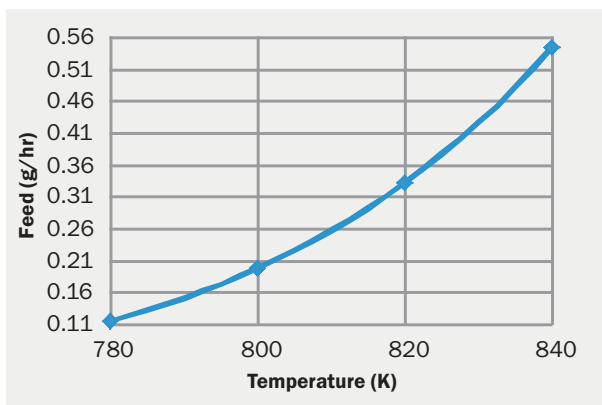


Fig.5: Variation of feed with source temperature.

Quantity and Quality of Product

Process of mass collection on product collector is shown in Fig.6.

Total mass of Yb deposited at product collector $P = \text{Non-selective pick-up} + \text{Collection of Yb-176 ions after ionization and extraction}$.

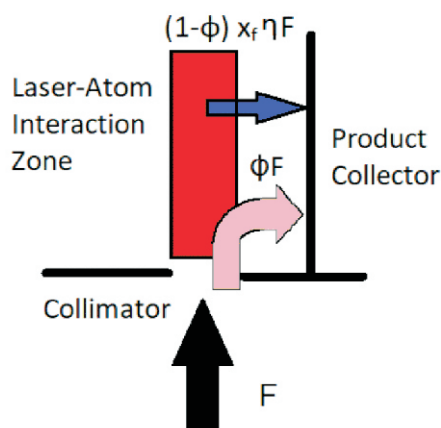


Fig.6: Deposition of material on product collector.

$$P = \Phi F + (1 - \Phi) \eta x_f = [\Phi + (1 - \Phi) \eta x_f] F \quad (14)$$

From equation-14 it is evident that product collection is linearly depends on stripping efficiency as well as non-selective pick-up for a given feed.

Deposition of only Yb-176 at product collector

$P^{Yb-176} = \text{Collection of Yb-176 due to non-selective pick-up} + \text{Collection of Yb-176 ions after ionization and extraction}$

$$P^{Yb-176} = [\Phi x_f + (1 - \Phi) \eta x_f] F \quad (15)$$

Concentration of Yb-176 at product collector is given by Eqn.16

$$x_p = \frac{P^{Yb-176}}{P} = \left[\frac{\Phi + (1 - \Phi) \eta}{\Phi + (1 - \Phi) \eta x_f} \right] x_f \quad (16)$$

Separation factor is given by Eqn.17

$$\beta_1 = \frac{x_p}{x_f} = \frac{\Phi + (1 - \Phi) \eta}{\Phi + (1 - \Phi) \eta x_f} \quad (17)$$

As per equation-16 product quality (x_p) depends only on non-selective pick-up and stripping efficiency for a given feed concentration. Variation of product quality is shown in Fig.7.

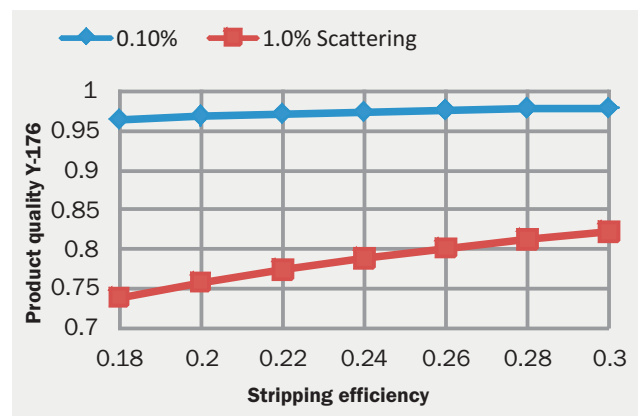


Fig.7: Variation of enrichment of Yb-176.

It is seen from Fig.6 that non-selective pick-up plays a major role to get high enrichment of more than 95% of Yb-176. Extraction geometry for product collection is designed such that non-selective pick-up comes down to 0.1% of feed.

Mass of 97.1% enriched product Yb-176 collected on product collector is shown in Fig.8 for various source temperatures (or feed) and stripping efficiencies. Production rate of 97.1% enriched isotope Yb-176 at a stripping efficiency 22% can be achieved in the range of 9 mg/hr to 16 mg/hr by

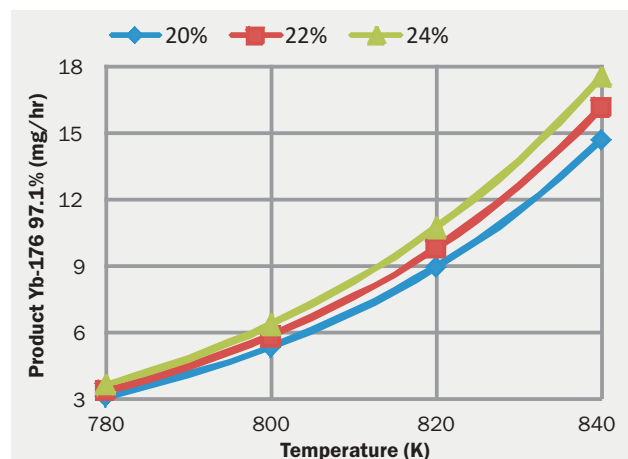


Fig.8: Variation of product mass (Eqn.14) for non-selective pick-up 0.1%.

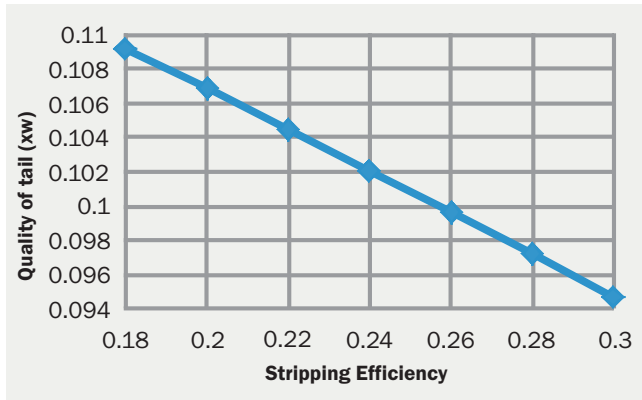


Fig.9: Variation of depletion of Yb-176 (Eqn.18).

controlling evaporation source temperature in between 820K to 840K. Hence, it is clear that production rate is very sensitive to the source temperature.

Mass depleted in Yb-176 collected at tail collector. Concentration of Yb-176 at tail collector is given by Eqn.18

$$x_w = \frac{(1 - \eta)x_f}{(1 - \eta x_f)} \quad (18)$$

Depletion factor is given by Eqn.19

$$\beta_2 = \frac{x_f}{x_w} = \frac{(1 - \eta x_f)}{(1 - \eta)} \quad (19)$$

Eqn.18 shows that depletion factor does not depend on scattering but decreases with increasing stripping efficiency as expected (Fig.9).

Comparison of Experimental Data with Analytical Values are listed in Table Below

Description	Experiment	Model
Temperature of crucible	810 K	820 K
Height of thickness monitor	240 mm	240 mm
Rate of deposit on thickness monitor	20 A/s	21.4 A/s
Non selective pick up (Scattering)	0.1%	0.1%
Stripping efficiency $\eta = \eta_a \times \eta_i \times \eta_{ex}$	18-28%	22%
Quantity of product	5.57 mg/hr	9.82 mg/hr
Quality of Yb-176 at product collector	97.1%	97.1%
Quality of Yb-176 at tail collector	9.12%	10.4%

Conclusions

Product quality 97.1% Yb-176 is achieved with stripping efficiency of 22% or more by restricting non-selective pick-up less than 0.1%. Product collection of 5.57mg/hr during experiment is less as compared to model value of 9.82 mg/hr. Moreover, concentration of Yb-176 at tail collector is less during experiment as compared to the model data. Both facts suggest that collection of enriched product is insufficient during experiment. So extraction mechanism and product collection geometry is to be improved.

Acknowledgements

The authors acknowledge all staff who involved in campaigns to perform Laser Isotope Separation of Yb-176. Authors also acknowledge G. K. Sahu, B. Jana and A.K. Singh of ATLA Facility, Beam Technology Development Group for their full support in analysis of experimental data.

Notations

- L = source length
- w = source width
- A = source area (wxL= 5mm x 100mm)
- T₀ = Source temperature
- P₀ = Source Pressure
- n₀ = number density at source
- M = Atomic weight of Yb=173
- R₀ = Universal gas constant = 8314 J/mole-K
- γ = Specific heat ratio = 5/3 for monotonic gas
- R = R₀/M = Characteristic gas constant = 48.05 J/kg-K
- A_v = Avogadro No
- k = R₀/A_v = Boltzman constant
- d = atomic diameter
- kn₀ = Knudsen number at source
- λ = Mean free path of atom
- S = thickness rate
- ρ = mass density of Yb,
- F = Feed or Throughput or mass supplied to atom-laser interaction volume
- P = Product mass collected at product collector
- W = Tail or waist mass collected at other location known as tail
- x_f, x_p, x_w : Concentration of Yb-176 in feed, product and tail respectively
- β₁ = Enrichment Factor = (x_p/x_f)
- β₂ = Depletion Factor = (x_f/x_w)
- Φ = Non selective pick-up (or Scattering efficiency) = Fraction mass of feed that reach to product collector without seeing laser
- η_a = Fraction of Yb-176 atoms in laser interaction zone available for atom –photon reaction
- η_i = Ionization efficiency= Fraction of Yb-176 atoms which ionized by laser in interaction zone
- η_{ex} = Extraction efficiency = Fraction of ionized Yb-176 atoms collected at product collector
- η = Stripping efficiency of Yb-176 ions (Ionization, extraction etc) = Overall fraction of Yb-176 atoms which go to laser interaction zone that collected at product collector
- η = η_i × η_{ex} × η_a
- n = Average no density of atom at laser interaction volume, atom/cc
- V = Volume of interaction zone (10 mm x 40mm x 100mm = 40 cc)
- v = Frequency of laser (rep rate) Hz = 12500 Hz
- t = Time for single pulse = 1/12500 sec = 80 x 10⁻⁶ sec

References

- [1] J. L. Parus, R. Mikolajczak, Beta-emitting radionuclides for peptide receptor radionuclide therapy. *Current Topics in Medical Chemistry* 2012, **12**(23), 2686-93.
- [2] A. M. R. Pillai, F. F. Knapp, Evolving Important Role of Lutetium-177 for Therapeutic Nuclear Medicine. *Current radio-pharmaceuticals*, 2015, **8**(2), 78-85.
- [3] V. A. Tarasov, O. I. Andreev et al., Production of No-Carrier Added Lutetium-177 by Irradiation of Enriched Yb-176, *Current Radiopharmaceuticals*, 2015, **8**, 95-106.
- [4] A. Dash, A. M. R. Pillai, Jr. F. F. Knapp, Production of Lu-177 for targeted radio nuclides therapy, *Available Options, Nucl Med Mol Imaging* 2015, **49** (2), 85-87.
- [5] W. V. Vogel, et al., Challenges and future option for the production of Lu-177, *Eur JI of Nuclear Medicine and Molecular Imaging*, 2021, **48**, 2329-2335.
- [6] R. John de Leater and Nino Buklic, The isotopic composition and atomic weight of ytterbium. June 2006 *International Journal of Mass Spectrometry*, **252**(3), 222-227.
- [7] Y. G. Toporov, et al., Production of high specific activity 177-Lu preparation using SM research reactor, 5th International Conference on Isotopes Brussels, Belgium, 25-29 April 2005, 10.
- [8] O. I. Andreev, et al., Production of highly enriched Yb-176 isotope in weight amounts by the atomic vapour laser isotope separation method, *Quantum Electronics*, 2006, **36**(1), 84-89.
- [9] H. Park, et al., Laser Isotope Separation of Yb-176 for medical Applications *Journal of Korean Physical Society* 2006, **49**(1), 382-386.
- [10] P. R. K. Rao, Laser Isotope Separation of Uranium, *Current Science*, 2003, **85**, 615.
- [11] Kundu S, et al., Summary of experimental results of RIS facility and Future projection, BARC/2020/R/006.
- [12] B. Dikshit, A. Sharma, Design and analytical evaluation of a new ion collection geometry for improvement in quantity and quality of product during laser isotope separation; *IEEE Trans Nuclear Science*, 2020, **67**(12), 2465-2473.
- [13] C. B. Alcock Vapor pressure of metallic elements, 2000, CRC Press LLC.
- [14] G. A. Bird, *Molecular Gas Dynamics and Direct Simulation of Gas flow*, Clarendon Press, Oxford, 1994.
- [15] J. Mukharjee, K. K. Mishra, L. M. Gantayet, Study of free jet expansion, BARC/1995/E/016.
- [16] A. Rosengard, Three Dimensional Free jet Flow from a finite Length Slit, *Rarefied Gas Dynamics*, ed. Muntze, et al., 1988, (16th RGD), 312-326.